NANO LETTERS

2008
Vol. 8, No. 7
2000-2005

Tuning of Solid Phase in Supracrystals Made of Silver Nanocrystals

A.-I. Henry, A. Courty, and M.-P. Pileni*

Laboratoire des Matériaux Mésoscopiques et Nanométriques, UMR CNRS 7070, Université Pierre et Marie Curie, BP 52, 4 place Jussieu, 75252 Paris Cedex 05, France

P.-A. Albouy

Laboratoire de Physique des solides, UMR CNRS 8502, Université Paris Sud, Bât 510, 91405 Orsay Cedex, France

J. Israelachvili

Department of Chemical Engineering and Materials Department, University of California, Santa Barbara, Santa Barbara, California 93106-5080

Received April 17, 2008; Revised Manuscript Received May 23, 2008

ABSTRACT

Decanethiol-passivated silver nanocrystals are shown, by small-angle X-ray diffraction, to organize into hexagonal close packed or face centered cubic (fcc) structures depending on the substrate temperature. When the nanocrystals are passivated by dodecanethiols, fcc and body centered cubic lattices as well as disordered arrangements are observed. The different crystalline phases correspond to thermodynamic equilibrium states. The passivant chain length is shown to control the interactions between the nanocrystals and consequently the superlattice structure.

Over the last 10 years, the superlattices of nearly spherical metallic and semiconductor nanocrystals have been intensively studied.[1–11] It has been shown that the main factors determining the preferred crystal structure of the superlattices are the chain length of the coating agent,[6,7] the morphology,[4,5] and the crystallinity[9] of the nanocrystals. The crystalline structure of the nanocrystal superlattices is usually either face-centered cubic (fcc) or hexagonal close packed (hcp). The nanoparticle superlattices constitute a novel type of artificial solid with properties determined by both individual nanoparticle building blocks and collective interactions.[8] Here, we show that the same silver nanocrystals (same size and crystallinity) passivated by decanethiols can adopt either hcp or fcc structures at a given pressure depending on the deposition temperature. However, when passivated by dodecanethiols (i.e., with two more carbon atoms) the phase diagram includes the dense fcc and the loose body centered cubic (bcc) lattices as well as disordered regions of random close packing (rcp). The two carbon atom difference in chain length is enough to totally modify the nanocrystal interactions leading to very different solid phases, all of which appear to be in the thermodynamic equilibrium state.

Silver nanocrystals (5.0 nm and 12% average diameter and size distribution, respectively) are synthesized in mixed functionalized reverse micelles as described elsewhere.[12,13] They are well crystallized. Indeed, a structural study has demonstrated that the nanocrystals are either cuboctahedra or decahedra and icosahedra.[14] They are coated by either decanethiol (C_{10}) or dodecanethiol (C_{12}) and are referred to $Ag-C_{10}$ and $Ag-C_{12}$, respectively. They are dispersed in decane and deposited on highly oriented pyrolitic graphite (HOPG) substrate by horizontally immersing the substrate in 200 μL of the colloidal solution (1.6×10^{11} nanocrystals/μL). The substrate temperature is controlled via a thermocouple-based module between 15 and 50 °C. Solvent evaporation takes place under a slow flow of nitrogen. Because of the high boiling point of decane (174 °C), its evaporation is slow and, depending on the substrate temperature, can take from 2 days to 3 weeks. After the solvent has evaporated, and regardless of the substrate temperature, scanning electron microscope imaging revealed a uniform film covering most of the substrate having an average thickness of about 1 μm. It corresponds to a three-dimensional (3D) film made of several supracrystals composed of more than a hundred nanocrystal layers.

* To whom correspondence should be addressed, pileni@sri.jussieu.fr.

10.1021/nl8010947 CCC: $40.75
Published on Web 06/10/2008

The relative ordering of the nanocrystals in the superlattices was investigated by small-angle X-ray diffraction (SAXRD) which was performed with a homemade system, with a copper anode.[15] The comparison of observed and calculated diffraction spot coordinates in the diffraction pattern enables determination of the crystal structure of the 3D nanocrystal assemblies. From the experimental spot coordinates and the sample−detector distance, we can determine the Bragg angle $2\theta_B$ and thus the modulus of the diffracted vector q from the Bragg relation. We can also determine the center-to-center interparticle distance from the position of the intense and well-defined Bragg reflections. The distances in the reciprocal space are converted into d_{hkl}-spacings using the formula $q = 2\pi/d_{hkl}$. The expressions for the projected q_x and q_y values are

$$q^x_{hkl} = \frac{2\pi}{D} l \sqrt{\frac{3}{8}}$$

and

$$q^y_{hkl} = \frac{2\pi}{D} \sqrt{\frac{4(h^2 + k^2 + hk)}{3}}$$

for hcp packing

$$q^x_{hkl} = \frac{2\pi}{D} \sqrt{\frac{h^2 + k^2 + l^2 - hk - kl - hl}{3}}$$

and

$$q^y_{hkl} = \frac{2\pi}{D} \frac{h + k + l}{\sqrt{6}}$$

for fcc packing, and

$$q^x_{hkl} = \frac{2\pi}{D} \frac{h + k}{2} \sqrt{\frac{3}{2}}$$

and

$$q^y_{hkl} = \frac{2\pi}{D} \sqrt{l^2 + \frac{(h - k^2)}{2}} \sqrt{\frac{3}{2}}$$

for bcc packing, D being the coated particle diameter.

The pattern obtained for Ag−C_{10} deposited at 15 °C (Figure 1A) shows two strong reflections (numbered 1 and 1′ in Figure 1A) normal to the substrate. The width of the first-order Bragg reflection is found nearly resolution limited (0.03 nm^{-1}) (inset I in Figure 1A), indicating long-range ordering of the nanocrystals perpendicular to the surface. Other less intense spots are observed on this pattern revealing a 3D long-range ordering within crystalline domains. The experimental and calculated diffraction spot coordinates agree very well with a hcp lattice (Figure S1 in Supporting Information). This agreement was further confirmed by the theoretical diffraction pattern calculated for spherical hard spheres (inset II in Figure 1A). The experimental center-to-center distance between silver nanocrystals, D, was calculated from the $d_{(002)}$spacing (Figure 2A) to give $D = d_{(002)}(3/2)^{1/2} = 7.1 \pm 0.6$ nm (Table 1). The deduced average interparticle spacing, δ, resulting from D is expressed as $\delta = D - 2R$, R being the average radius of the silver nanocrystals determined from transmission electron microscopy images. The interparticle spacing δ was found to be 2.1 ± 0.6 nm, i.e., less than twice the thickness of a decanethiol self-assembled monolayer (SAM) on a flat substrate.[16] This suggests that long-range ordering arises from the interdigitation of chains on neighboring particles.

On increase of the substrate (and deposition) temperature to 25 °C, the diffraction pattern of the Ag−C_{10} nanocrystal film has changed significantly (Figure 1B). It is now a typical fcc lattice with the (111) plane lying parallel to the substrate.[15] The width of the first-order Bragg reflection is nearly resolution limited (0.03 nm^{-1}) (inset I in Figure 1B), indicating long-range ordering of the nanocrystals perpendicular to the surface. The elongation of the diffraction spots (numbered 2 and 3 in Figure 1B) is attributed to stacking faults in the supracrystals in agreement with the simulated diffraction pattern in inset II of Figure 1B. Note that the rings observed in the diffraction pattern indicate that the supracrystals are not all oriented in the (111) direction.

On increase of the substrate temperature to 35 and 50 °C (panels C and D of Figure 1), the number of stacking faults decreases and the diffraction spots become more well-defined (less elongated) and more intense. At 50 °C (Figure 1C) a less intense and thinner ring is observed indicating that a larger number of the supracrystals have the same (111) orientation than those obtained at 25 and 35 °C. From 25 to 35 °C, the silver nanocrystals center-to-center distance D deduced from the profiles (insets I in panels B−D of Figure 1) and calculated from the d_{111} spacing ($D = d_{(111)}(3/2)^{1/2}$) (Figure 2B) varies from 7.2 ± 0.3 to 7.1 ± 0.3 nm (Table 1). Thus the D value does not vary with the substrate temperature or the type of organization (fcc or hcp) and implies chain interdigitation.

Thus, the same nanocrystals dispersed in a given solvent (decane) organize into either hcp or fcc supracrystals. These crystalline structures correspond to equilibrium states, as they do not depend on the solvent evaporation rate. Indeed, depositions and evaporations at 25 °C, whether under a slow flow of nitrogen gas or under an atmosphere rich in decane, leading to evaporation times of 2 and 20 days, respectively, yielded similar SAXRD patterns typical of fcc packing. fcc and hcp are the most efficient packing for hard spheres. The hcp−fcc transition is energetically controlled.[17–19] hcp has indeed a lower total Lennard-Jones energy than fcc because in the ABAB stacking of hcp the next-nearest neighbor spheres are closer together than in ABCABC stacking of fcc. Recently, a small difference in free energy between fcc and hcp of around $10^{-3} k_B T$ was calculated.[20] Our results show that an increase of the substrate temperature from 15 to 25 °C is enough to induce the hcp-to-fcc transition. The increase of the temperature modifies the steric repulsions between the alkyl chains as it modifies their mobility.[21] This probably changes the free energy of the system and thus induces the hcp−fcc phase transition.

We now consider the same nanocrystals but coated with dodecanethiol (Ag−C_{12}) instead of decanethiol (Ag−C_{10}) and dispersed in the same solvent, decane, as previously. The SAXRD patterns are markedly different (Figure 3). At 15 °C, the diffraction pattern shows a halo at 1 nm^{-1} with an estimated intrinsic width of $\delta q_{1/2} = 0.25$ nm^{-1} which is larger

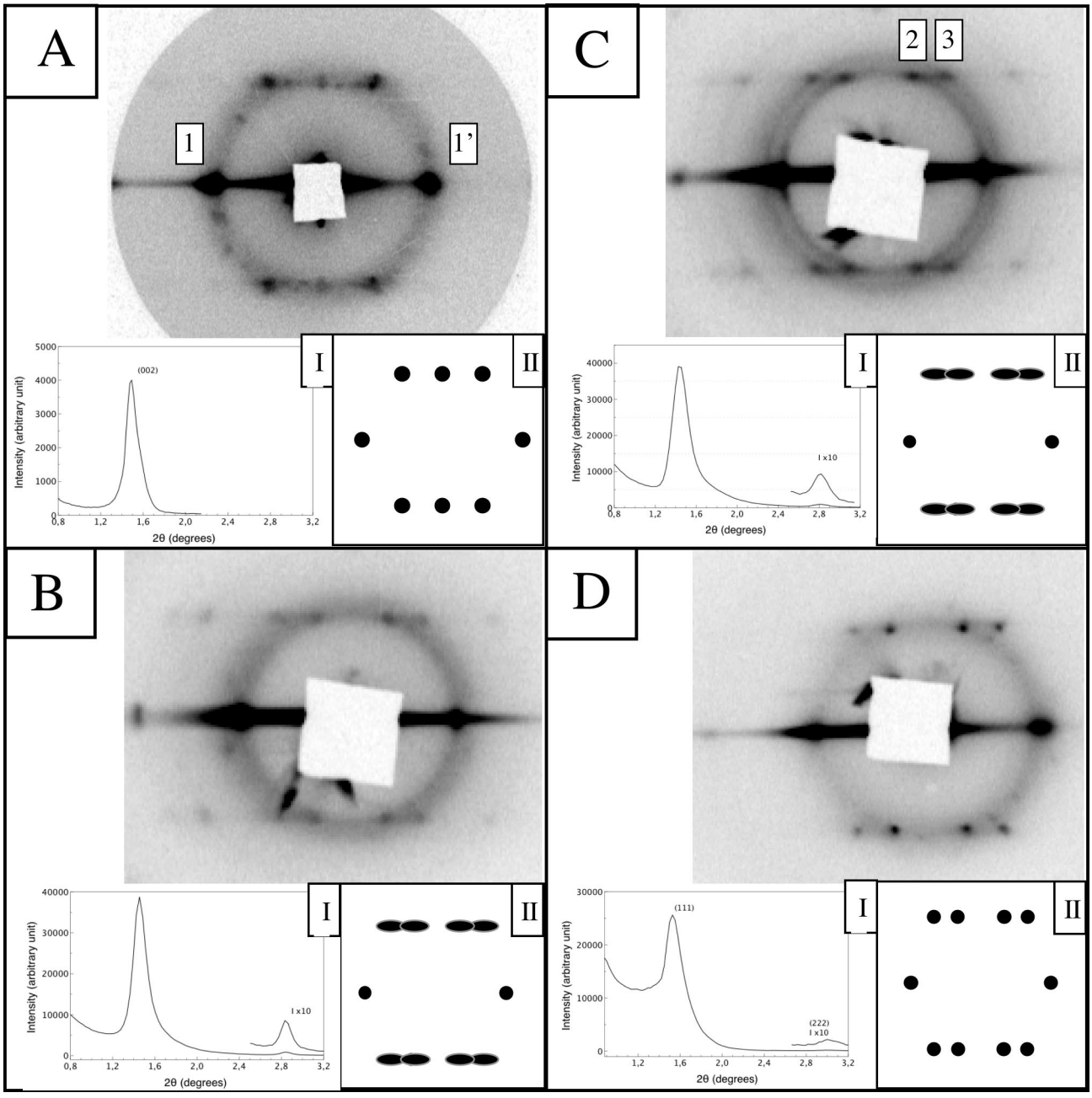

Figure 1. Small-angle X-ray diffraction patterns corresponding to Ag−C_{10} nanocrystals initially dispersed in decane, evaporated at 15 °C (A), 25 °C (B), 35 °C (C), and 50 °C (D). The insets I and II present the corresponding profiles and simulated diffraction patterns, respectively.

than the experimental resolution (0.03 nm^{-1}) (Figure 3A and inset I). The corresponding correlation length is crudely estimated at 11 nm using the Scherrer formula ($0.888\pi/\delta q_{1/2}$). This behavior indicates that the silver nanocrystals are random close packed (rcp), and we calculate a mean interparticle distance of 7.4 ± 0.4 nm (Table 1).

On increase of the substrate temperature to 25 °C, the diffraction pattern is clearly typical of 3D hcp supracrystals (Figure 3B and inset II). The corresponding profile shows a first-order Bragg reflection, nearly resolution limited (0.03 nm^{-1}) (inset I in Figure 3B), and the diffraction spots are well-defined and intense; both of these indicate long-range ordering. The D value calculated from the d_{002} spacing (Figure 2A) gives $D = d_{(002)}(3/2)^{1/2} = 7.4 \pm 0.1$ nm (Table 1). The deduced average interparticle spacing resulting from D is found to be 2.4 ± 0.6 nm, which again implies chain interdigitation. It is higher than the one obtained with Ag−C_{10} at the same substrate temperature (Table 1). The increase in the chain length ($\Delta L = 0.6$ nm) can explain this result.[15]

At 35 °C, the diffraction pattern displays several diffraction spots typical of a close-packed structure (Figure 3C). The large elongation of the spots is due to a large number of stacking faults according to the corresponding simulated pattern (inset II in Figure 3C). For a large number of stacking faults in the supracrystals, it is obviously difficult to distinguish an fcc from an hcp packing. Nevertheless, whatever the number of stacking faults, the long-range order

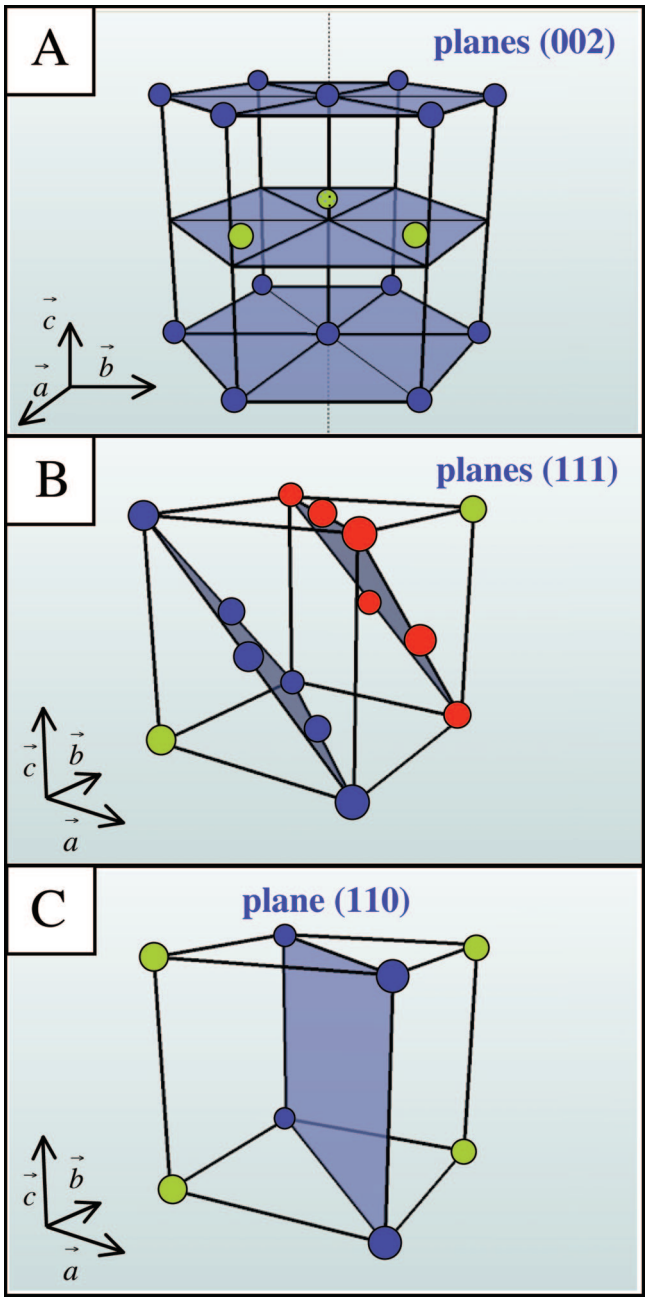

Figure 2. Schematic representation of sphere packing into (A) hexagonal-close-packed lattice, (B) face-centered-cubic lattice, and (C) body-centered-cubic lattice. In blue are represented the planes of highest density in the lattices A, B, and C.

Table 1. Packing and Corresponding Center-to-Center Distance D in Ag−C_{10} and in Ag−C_{12} Supracrystals as a Function of the Substrate Temperature

	15 °C	25 °C	35 °C	50 °C
Ag−C_{10} packing	hcp	fcc	fcc	fcc
D (nm)	7.1 ± 0.6	7.2 ± 0.3	7.2 ± 0.3	7.1 ± 0.3
Ag−C_{12} packing	rcp	hcp	dense packing	bcc
D (nm)	7.4 ± 0.4	7.4 ± 0.1	8.4 ± 0.1	7.9 ± 0.1[a]

[a] Note that for bcc packing, the distance D is the minimal distance calculated in the (110) plane.

remains the same. Indeed, the width of the first-order Bragg reflection remains nearly resolution limited (inset I in Figure 3C). The interparticle distance D has increased to 8.4 ± 0.1 nm and is probably due to the numerous stacking faults.

On increase of the substrate temperature to 50 °C, the diffraction pattern markedly changes and displays diffraction spots attributed to a bcc lattice (Figure 3D and Figure S2 in the Supporting Information). This is confirmed by the corresponding calculated diffraction pattern in inset II of Figure 3D. Note that a large and diffuse ring is also observed in the diffraction pattern indicating that some 3D assemblies on the substrate are disordered. The minimal distance D_{min} between nanocrystals in a bcc packing is deduced from the profiles (inset I in Figure 3D) as $D_{min} = d_{(110)}(3/2)^{1/2} = 7.9 \pm 0.1$ nm (Table 1), where $d_{(110)}$ is the interplane distance between the (110) planes (Figure 2C).

The solid phase diagram of Ag−C_{12} is clearly different from the one of Ag−C_{10} and includes rcp, fcc, and bcc lattices. The rcp−fcc−bcc transitions are tuned by changing the substrate temperature during the solvent evaporation. Many soft spheres systems as, for example, crystals of self-assembled spherical micelles and block copolymers, are reported to form non-close-packed lattices including bcc, body-centered-orthorhombic (bco), and diamond lattices.[18,22,23] The stability of the coated silver nanocrystals depends not only on the hard-core repulsion between the cores but also on the interaction between the thiol coronas. The soft corona is known to favor structures that minimize the interfacial energy favoring the loose structure (bcc), and the hard cores are known to favor lattices with high packing fractions.[18] The true ground state is determined by balancing these two competing tendencies. The presence of hydrocarbon chains between the particles clearly modifies the delicate balance between these interactions. Indeed, the interdigitation between the alkyl chains reduces their orientational entropy within the corona, which gives rise to a short-range repulsive interaction. Nanocrystal assembly is controlled primarily by hard-core repulsion.[18] In this case, in a first approximation, dense lattices such as fcc or hcp are favored. When the interparticle distances D increase, the repulsive interactions, which are at short range, vanish. In this case, the assembly becomes controlled by the soft coronas and loose lattices of more open lattices such as the bcc are favored. This suggests that Ag nanocrystals form dense superlattices by virtue of the interdigitation of the neighboring alkyl chains. Temperature-dependent infrared spectroscopy analysis performed by Pradeep et al. shows that the dynamic of the C_{12} chains arises abruptly at the melting temperature (52 °C).[21] At this temperature, 70% of the chains are found to be dynamic. Thus they cannot take part to the interdigitation and induce the formation of loose Ag−C_{12} superlattices. This is in agreement with the calculations performed by Robbins et al. which show that even when the stable solid phase is fcc below the melting temperature, the bcc lattice is favored in the liquid phase.[24] The dynamics of shorter chains evolves progressively with the temperature. Pradeep et al. show indeed that C_8 and C_6 chains are not dynamics at room temperature.[21] When the temperature increases, the proportion of alkyl chains participating to the dynamics increases, and at 127 °C all the chains participate to the dynamics.

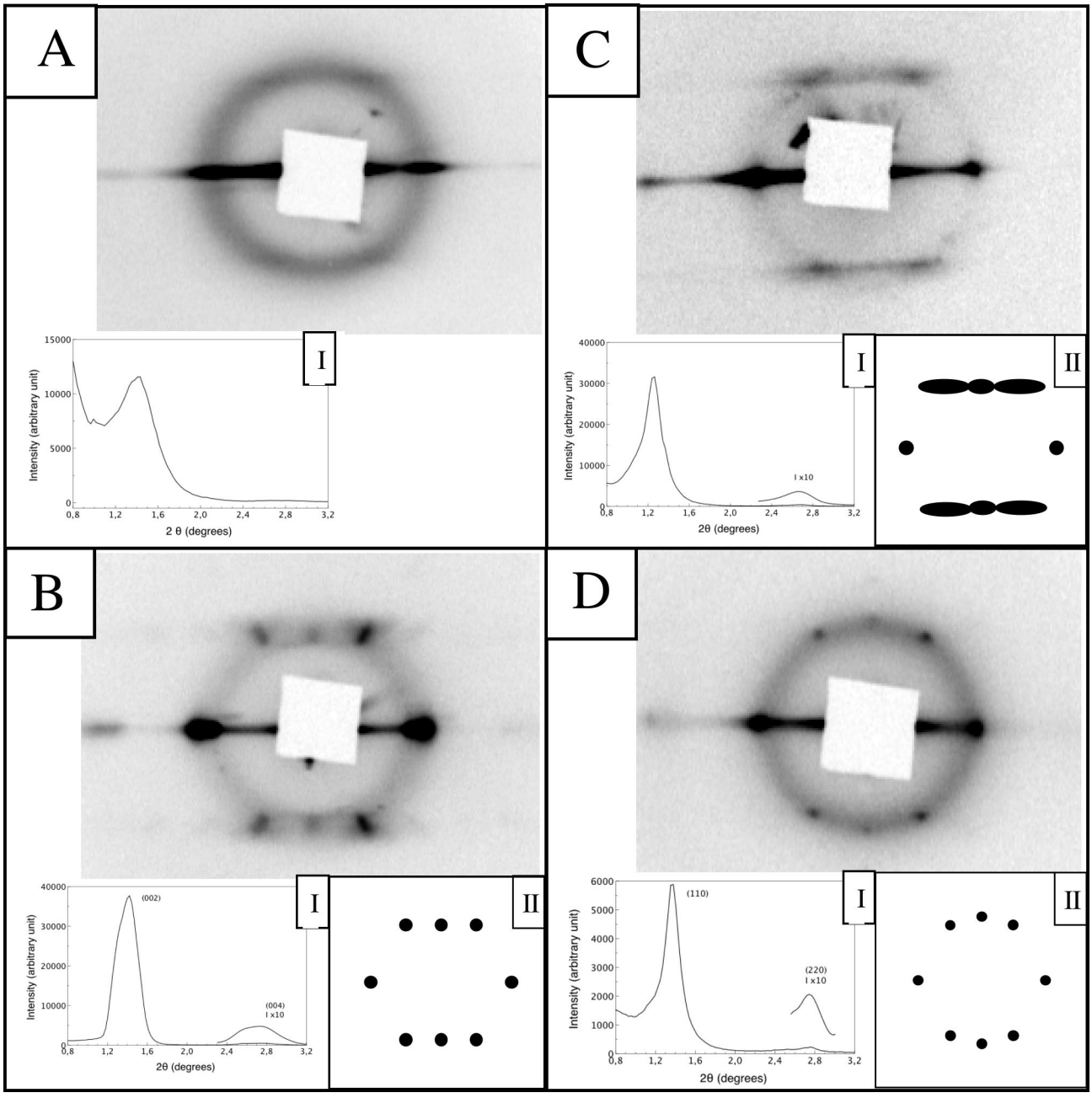

Figure 3. Small-angle X-ray diffraction patterns corresponding to $Ag-C_{12}$ nanocrystals initially dispersed in decane, evaporated at 15 °C (A), 25 °C (B), 35 °C (C), and 50 °C (D). The insets I and II present the corresponding profiles and simulated diffraction patterns, respectively.

These results are in agreement with our observation of dense superlattices (hcp, fcc) until 50 °C for $Ag-C_{10}$ and until 35 °C for $Ag-C_{12}$. Above 35 °C, more open $Ag-C_{12}$ superlattices as the bcc are observed.

In order to probe the effect of the alkyl chain length on the crystalline phase of silver supracrystals, we have performed similar experiments with silver nanocrystals coated by either tetradecanethiols ($Ag-C_{14}$) or octanethiols ($Ag-C_8$). The presence of defects at the end of the C_{14} chains prevents the formation of supracrystals. The SAXRD patterns show a halo characteristic of disordered arrangements. This is in agreement with previous results obtained by Motte et al. with Ag_2S-C_{14} nanocrystals.[16] The silver nanocrystals coated by C_8 chains coalesce rapidly and are thus not stable enough to form supracrystals.

In conclusion, the alkyl chain length and the deposition temperature are shown to be critical parameters for the solid phase diagram of silver supracrystals. Depending on both parameters, the crystalline phase diagram of nanocrystal superlattices includes dense (fcc, hcp) and loose (bcc) lattices. A difference in the alkyl chain length as small as two carbon atoms is shown to have a strong effect on these crystalline structures. These are attributed to equilibrium states as they do not depend on the solvent evaporation rate. The concept of silver nanocrystals as "hard cores" with a "soft corona" is introduced in order to describe the interactions between

the nanocrystals. We show that the balance between the hard-core repulsion and the short-range repulsive interaction of the alkyl chains (which can be tuned by their length) determines whether nanocrystals form dense or loose lattices.

Acknowledgment. We acknowledge fruitful discussions with Professor Z. L. Wang of the Georgia Institute of Technology, Atlanta, GA.

Supporting Information Available: Indexes of SAXRD patterns for hcp and bcc packing. This material is available free of charge via the Internet at http://pubs.acs.org.

References

(1) Harfenist, S. A.; Wang, Z. L.; Whetten, R. N.; Vezmar, I.; Alvarez, M. M. Three-dimensional hexagonal close-packed superlattice of passivated Ag nanocrystals. *Adv. Mater.* **1997**, *9*, 817.
(2) Collier, C. P.; Vossmeyer, T.; Heath, J. R. Nanocrystal superlattices. *Annu. Rev. Phys. Chem.* **1998**, *49*, 371.
(3) Korgel, B. A.; Fullam, S.; Connoly, S.; Fitzmaurice, D. Assembly and self-organization of silver nanocrystal superlattices: ordered "soft spheres". *J. Phys. Chem. B* **1998**, *102*, 8379.
(4) Wang, Z. L.; Harfenist, S. A.; Whetten, R. L.; Bentley, J.; Evans, N. D. Bundling and interdigitation of adsorbed thiolate groups in self-assembled nanocrystal superlattices. *J. Phys. Chem.* **1998**, *102*, 3068.
(5) Wang, Z. L. Structural analysis of self-assembling nanocrystal superlattices. *Adv. Mater.* **1998**, *1*, 13.
(6) Whetten, R. L.; Shafgullin, M. N.; Khoury, J. T.; Shaaf, T. G.; Vezmar, I.; Alvarez, M. M.; Wilkinson, A. Crystal structures of molecular gold nanocrystal arrays. *Acc. Chem. Res.* **1999**, *32*, 397.
(7) Korgel, B. A.; Fitzmaurice, D. Small-angle x-ray scattering study of silver-nanocrystal disorder-order phase transitions. *Phys.Rev. B* **1999**, *59*, 14191.
(8) Pileni, M.-P. Nanocrystal self-assemblies: fabrication and collective properties. *J. Phys. Chem. B* **2001**, *105*, 3358.
(9) Stoeva, S. I.; Prasad, B. L. V.; Uma, S.; Stoimenov, P. K.; Zaikovski, V.; Sorensen, C. M.; Klabunde, K. J. Face-centered cubic and hexagonal closed-packed nanocrystal superlattices of gold nanoparticles prepared by different methods. *J. Phys. Chem. B* **2003**, *107*, 7441.
(10) Pileni, M.-P. Self-assembly of inorganic nanocrystals: fabrication and collective intrinsic properties. *Acc. Chem. Res.* **2007**, *40*, 685.
(11) Talapin, D. V.; Shevchenko, E. V.; Murray, C. B.; Titov, A. V.; Kral, P. Dipole-dipole interactions in nanoparticle superlattices. *Nano Lett.* **2007**, *7*, 1213.
(12) Taleb, A.; Petit, C.; Pileni, M.-P. Synthesis of highly monodisperse silver nanoparticles from AOT reverse micelles: a way to 2D and 3D self-organization. *Chem. Mater.* **1997**, *9*, 950.
(13) Courty, A.; Henry, A.-I.; Goubet, N.; Pileni, M.-P. Large triangular single crystals formed by mild annealing of self-organized silver nanocrystals. *Nat. Mater.* **2007**, *6*, 900.
(14) Courty, A.; Lisiecki, I.; Pileni, M.-P. Vibration of self-organized silver nanocrystals. *J. Chem. Phys.* **2002**, *116*, 8074.
(15) Courty, A.; Mermet, A.; Albouy, P.-A.; Duval, E.; Pileni, M.-P. Vibrational coherence of self-organized silver nanocrystals in fcc supra-crystals. *Nat. Mater.* **2005**, *4*, 395.
(16) Motte, L.; Pileni, M.-P. Self-assemblies of silver sulfide nanocrystals: influence of length of thio-alkyl chains used as coating agent. *Appl. Surf. Sci.* **2000**, *164*, 60.
(17) Mau, S.-C.; Huse, D. A. Stacking entropy of hard-sphere crystals. *Phys. Rev. E* **1999**, *59*, 3396.
(18) Ziherl, P.; Kamien, R. D. Maximizing entropy by minimizing area: towards a new principle of self-organization. *J. Phys. Chem. B* **2001**, *105*, 10147.
(19) Koch, H.; Radin, C.; Sadun, L. Most stable structure for hard spheres. *Phys. Rev. E* **2005**, *72*, 016708-1.
(20) Bolhuis, P. G.; Frenkel, D.; Mau, S.-C.; Huse, D. A. Entropy difference between crystal phases. *Nature* **1997**, *388*, 235.
(21) Pradeep, T.; Mitra, S.; Sreekumaran Nair, A.; Mukhopadhyay, R. Dynamics of alkyl chains in monolayer-protected Au and Ag clusters and silver thiolates: a comprehensive quasielastic neutron scattering investigation. *J. Phys. Chem. B* **2004**, *108*, 7012.
(22) Balagurusamy, V. S. K.; Ungar, G.; Percec, V.; Johansson, G. Rational Design of the First Spherical Supramolecular Dendrimers Self-Organized in a Novel Thermotropic Cubic Liquid-Crystalline Phase and the Determination of Their Shape by X-ray Analysis. *J. Am. Chem. Soc.* **1997**, *119*, 1539.
(23) Hamley, I. W.; Daniel, C.; Mingvanish, W.; Mai, S.-M.; Booth, C.; Messe, L.; Ryan, A. J. From hard spheres to soft spheres: the effect of copolymer composition on the structure of micellar cubic phases formed by diblock coplymers in aqueous solution. *Langmuir* **2000**, *16*, 2508.
(24) Robbins, M. O.; Kremer, K.; Grest, G. S. Phase diagram and dynamics of Yukawa systems. *J. Chem. Phys.* **1988**, *88*, 3286.

NL8010947